

Convergence Properties of the Effective Theory for Trapped Bosons

S. Tölle,^{*} H.-W. Hammer,[†] and B. Ch. Metsch[‡]

*Helmholtz-Institut für Strahlen- und Kernphysik and Bethe Center for Theoretical Physics,
Universität Bonn, 53115 Bonn, Germany*

(Dated: July 6, 2018)

Abstract

We investigate few-boson systems with resonant interactions in a narrow harmonic trap within an effective theory framework. The size of the model space is identified with the effective theory cutoff. In the universal regime, the interactions of the bosons can be approximated by contact interactions. We investigate the convergence properties of genuine and smeared contact interactions as the size of the model space is increased and present a detailed error analysis. The spectra for few-boson systems with up to 6 identical particles are calculated by combining extrapolations in the cutoff and in the smearing parameter.

arXiv:1210.8373v1 [cond-mat.quant-gas] 31 Oct 2012

^{*} toelle@hiskp.uni-bonn.de

[†] hammer@hiskp.uni-bonn.de

[‡] metsch@hiskp.uni-bonn.de

I. INTRODUCTION

Few-body systems with resonant interactions show universal properties independent of the details of the interaction at short distances [1]. If the scattering length a is much larger than the range of the interaction r_0 , the underlying interaction can be approximated by an effective theory with contact interactions. In the two-body system, the universal properties include the existence of a shallow dimer with binding energy $E_2 \approx -\hbar^2/(ma^2)$, if a is positive. In the three-body system, the Efimov effect then generates a geometric spectrum of three-body bound states [2]:

$$E_3^{(n)} = -(e^{-2\pi/s_0})^n \hbar^2 \kappa_*^2 / m, \quad n = 0, 1, 2, \dots \quad (1)$$

where $s_0 = 1.00624\dots$ and κ_* is the binding momentum of the lowest Efimov state. This spectrum shows a discrete scaling symmetry which corresponds to a renormalization group limit cycle [3]. Recent theoretical studies have shown that these universal properties also hold for the four-body system. In particular, there is a pair of universal four-body states associated with every Efimov state [4, 5]. Moreover, universal cluster states have been predicted in five-, six- and possibly higher-body systems as well [6–9]. Using Feshbach resonances, the two-, three-, four- and five-body states have been confirmed in a ultracold atomic gases in a variety of experiments with different atom species [10–12].

These experiments were carried out in a regime where the influence of the trap on the few-body spectra could be neglected. However, the trap also offers new possibilities to modify the properties of few-body systems. In particular, a narrow harmonic confinement modifies the spectrum. Microtraps with a small number of atoms offer the opportunity to study the transition from few- to many-body systems in a controlled environment.

Many studies have focused on fermions in the unitary regime in a harmonic trap where the Efimov effect does not occur (see Ref. [13] for a review of this work). Here, we focus on the case of spinless bosons. The 2-body problem of spinless bosons with contact interactions in an isotropic harmonic trap was solved analytically by Busch et al. [14]. The corresponding 3-body problem was first solved by Jonsell et al. [15]. Werner and Castin calculated the complete 3-body spectrum in the unitary limit of infinite scattering length and provided a semi-analytic solution [16]. More recent work has focused on the universality of the two-body spectrum [17, 18], the extension to heteronuclear systems [19] and anisotropic traps [20, 21], and the interpretation of the scattering-length dependence of the level structure in terms of the Zel'dovich effect [22].

In this work, we investigate universal few-body physics in harmonic confinement for up to six bosons using an effective theory framework. Our strategy follows Stetcu et al. [23–25], where an effective theory for short-range nuclear forces in the framework of the no-core shell model was formulated. The effective interactions were defined within a finite model space with a cutoff N on the basis functions. In previous work [26], we have performed a systematic study of the spectra of three- and four-body systems in the vicinity of the unitary limit at leading order in the effective theory. In this paper, we extend our calculations to six bodies. The running of the coupling constants for two- and three-body interactions with the cutoff N is investigated in detail. Moreover, we introduce smeared contact interactions. We compare the convergence of the effective theory as the size of the model space is increased for exact and smeared contact interactions and discuss different strategies to remove the regulator. Finally, spectra for A -boson systems with up to six bodies are calculated using a combined extrapolation in N and the smearing parameter ϵ .

II. THEORETICAL FRAMEWORK

We investigate few-boson systems with resonant two-body interactions characterized by a large S-wave scattering length a in a harmonic trap using an effective theory with contact interactions. The contact interactions lead to ultraviolet divergences which have to be renormalized by fixing one two-body energy (or, equivalently the scattering length a) and a three-body energy [3, 27]. Since the trap only modifies the infrared properties of the system, the renormalization of the contact interactions is the same as in free space. We stay at leading order in the effective theory. (See Refs. [28, 29] for an explicit calculation of effective range corrections for two-component fermions.) Higher-order corrections are suppressed by κR where $\kappa = \sqrt{m|E|}$ is a typical momentum and R is the range of the interaction. For broad Feshbach resonances R is given by the van der Waals length l_{vdW} . For trapped systems, there are also corrections of order R/β , where $\beta = \sqrt{\hbar/(m\omega)}$ is the oscillator length. As we will discuss below, there are additional corrections if the two- and three-body renormalization energies E_2 and E_3 are very different.

We implement this effective theory in a Hamiltonian framework. For a system of A bosons in an isotropic harmonic oscillator potential (HOP) at leading order the Hamiltonian can be written as

$$H = \sum_{i=1}^A \left(\frac{|\vec{p}_i|^2}{2m} + \frac{1}{2}m\omega^2|\vec{x}_i|^2 \right) + g^{(2)} \sum_{i<j}^A V_{ij} + g^{(3)} \sum_{i<j<k}^A W_{ijk}, \quad (2)$$

where V and W are two- and three-body contact interactions, m is the mass of the bosons, and ω is the trapping frequency. In the following, all lengths are rescaled with the oscillator length $\beta = \sqrt{\hbar/(m\omega)}$ for convenience. Since the interactions are Galilei invariant and the HOP allows to separate the center of mass motion, the problem is transformed to an $(A-1)$ -body problem in Jacobi coordinates \vec{s}_n and a one body problem in \vec{R} , where

$$\vec{s}_n = \frac{1}{\beta\sqrt{(n+1)n}} \left(\sum_{j=1}^n \vec{x}_j - n\vec{x}_{n+1} \right), \quad \vec{R} = \frac{1}{\beta\sqrt{A}} \left(\sum_{j=1}^A \vec{x}_j \right), \quad (3)$$

with the property $\sum_{j=1}^A |\vec{x}_j|^2 = \beta^2 \left(\sum_{n=1}^{A-1} |\vec{s}_n|^2 + |\vec{R}|^2 \right)$.

The Hamiltonian (2) has to be regularized since it is not self-adjoint. Hence the Hilbert space is restricted to the model space consisting of the linear hull of oscillator states $\{\otimes_{i=1}^{A-1} |n_i l_i m_i\rangle\}$ with eigenvalues $\sum_{i=1}^{A-1} \hbar\omega(2n_i + l_i + \frac{3}{2}) \leq \hbar\omega(N + (A-1)\frac{3}{2})$ [30]. In order to match the results in the model space to the full Hilbert space results, the coupling constants $g^{(2)}$ and $g^{(3)}$ are renormalized (see Sec. II B). We identify N with the ultraviolet cutoff of our effective theory. The coupling constants $g^{(2)}$ and $g^{(3)}$ are fixed by matching to a two- and a three-body energy, respectively, and run with the cutoff N . In free space one usually uses a momentum cutoff Λ to regularize the resulting integral equation and finds a linear dependence of observables on $1/\Lambda$ in first order of perturbation theory. Because of the relation $p \propto \sqrt{E}$ between momentum p and energy E , we expect errors in the eigenenergies in the trap of order $1/\sqrt{N + (A-1)3/2}$.

In contrast to the momentum cutoff Λ used in free space, the regulator N also implies an infrared cutoff. In the literature, there are two definitions of the IR-cutoff for an oscillator basis. Both the expression $\beta/\sqrt{N + (A-1)3/2}$ [31, 32], which quantifies the maximum size of structures that can be captured in the given basis, or the oscillator length β itself [33] have

been interpreted as an IR-cutoff. In our calculations, the harmonic oscillator represents a physical trap and thus β is a physical parameter. The trap acts like a finite box that confines the system. In this case, only the first definition is sensible and we expect errors of order $1/\sqrt{N + (A - 1)3/2}$ from the infrared cutoff. These errors have the same scaling behavior with N as the errors from the ultraviolet cutoff and vanish for $N \rightarrow \infty$.

In our previous work, we found that the convergence to the results in the full Hilbert space is slow due to the irregularity of the δ -distribution in the parametrization of the genuine contact interactions [26]. For the cutoff dependence to become insignificant, values for $1/\sqrt{N}$ of order 0.1 or smaller have to be reached. For four- and higher-body states such low values can in general not be obtained. The eigenenergies are estimated by extrapolation of results for finite N to $N \rightarrow \infty$.

Here, we investigate a second possibility. The convergence can be improved by smearing the contact interactions. We keep the separability of the interaction and approximate the contact interactions by narrow Gaussians with width ϵ . More specifically, the separable two-body contact interaction

$$\langle \vec{s} | V | \vec{s}' \rangle = \delta^{(3)}(\vec{s}) \delta^{(3)}(\vec{s} - \vec{s}') = \delta^{(3)}(\vec{s}) \delta^{(3)}(\vec{s}') \quad (4)$$

is substituted by

$$\langle \vec{s} | V_\epsilon | \vec{s}' \rangle = (2\pi\epsilon^2)^{-3/2} e^{-|\vec{s}|^2/(2\epsilon^2)} (2\pi\epsilon^2)^{-3/2} e^{-|\vec{s}'|^2/(2\epsilon^2)}, \quad (5)$$

and the three-body contact interaction

$$\langle \vec{s}_1, \vec{s}_2 | W | \vec{s}'_1, \vec{s}'_2 \rangle = \delta^{(3)}(\vec{s}_1) \delta^{(3)}(\vec{s}'_1) \delta^{(3)}(\vec{s}_2) \delta^{(3)}(\vec{s}'_2) \quad (6)$$

is replaced by

$$\langle \vec{s}_1, \vec{s}_2 | W_\epsilon | \vec{s}'_1, \vec{s}'_2 \rangle = (2\pi\epsilon^2)^{-6} e^{-(|\vec{s}_1|^2 + |\vec{s}_2|^2 + |\vec{s}'_1|^2 + |\vec{s}'_2|^2)/(2\epsilon^2)}. \quad (7)$$

The case of contact interactions is then recovered in the limit $\epsilon \rightarrow 0$.

A. Matrix elements

The eigenenergies are determined by diagonalization of the Hamiltonian matrix in an angular-momentum-coupled basis of oscillator states. For contact interactions as well as smeared contact interactions one can easily find the matrix elements for the oscillator basis functions

$$\phi_{n_1 l_1 m_1}(\vec{s}_1) = R_{n_1 l_1}(|\vec{s}_1|) Y_{l_1 m_1}(\Omega) = \langle \vec{s}_1 | n_1 l_1 m_1 \rangle. \quad (8)$$

For two-body contact interactions, we have

$$\langle n_1 l_1 m_1 | V | n'_1 l'_1 m'_1 \rangle = \phi_{n_1 0}(0) \phi_{n'_1 0}(0) \delta_{l_1 0} \delta_{l'_1 0}, \quad (9)$$

where

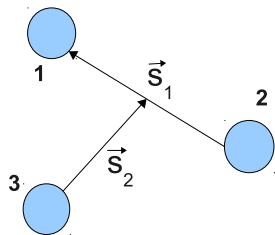
$$\phi_{n0}(0) = \frac{1}{\pi^{3/4}} \left(\frac{\Gamma(n + \frac{3}{2})}{\Gamma(\frac{3}{2}) \Gamma(n + 1)} \right)^{1/2} = \left(\frac{(2n + 1)!!}{\pi^{3/2} n! 2^n} \right)^{1/2}. \quad (10)$$

For the smeared two-body contact interaction, we obtain according to Appendix B

$$\langle n_1 l_1 m_1 | V_\epsilon | n'_1 l'_1 m'_1 \rangle = \frac{1}{(1 + \epsilon^2)^3} \left(\frac{1 - \epsilon^2}{1 + \epsilon^2} \right)^{n_1 + n'_1} \phi_{n_1 0}(0) \phi_{n'_1 0}(0) \delta_{l_1 0} \delta_{l'_1 0} . \quad (11)$$

The three-body interactions are determined in a coupled scheme, i.e. both angular momenta are coupled to a total angular momentum with Clebsch-Gordan coefficients,

$$[\phi_{n_1 l_1}(\vec{s}_1) \otimes \phi_{n_2 l_2}(\vec{s}_2)]_M^L = \langle \vec{s}_1, \vec{s}_2 | n_1 l_1, n_2 l_2, LM \rangle . \quad (12)$$



$$\begin{aligned} \vec{s}_1 &= \frac{1}{\beta\sqrt{2}}(\vec{x}_1 - \vec{x}_2) , \\ \vec{s}_2 &= \frac{1}{\beta\sqrt{6}}(\vec{x}_1 + \vec{x}_2 - 2\vec{x}_3) , \\ \vec{R} &= \frac{1}{\beta\sqrt{3}}(\vec{x}_1 + \vec{x}_2 + \vec{x}_3) . \end{aligned}$$

Figure 1. Set of Jacobi coordinates for the three-body system.

We find for the three-body contact interactions in Jacobi coordinates \vec{s}_1 and \vec{s}_2

$$\langle n_1 l_1, n_2 l_2, LM | W | n'_1 l'_1, n'_2 l'_2, L' M' \rangle = \phi_{n_1 0}(0) \phi_{n'_1 0}(0) \phi_{n_2 0}(0) \phi_{n'_2 0}(0) \delta_{l_1 0} \delta_{l'_1 0} \delta_{l_2 0} \delta_{l'_2 0} , \quad (13)$$

and finally for the smeared three-body contact interaction

$$\begin{aligned} \langle n_1 l_1, n_2 l_2, LM | W_\epsilon | n'_1 l'_1, n'_2 l'_2, L' M' \rangle = \\ \frac{1}{(1 + \epsilon^2)^6} \left(\frac{1 - \epsilon^2}{1 + \epsilon^2} \right)^{n_1 + n_2 + n'_1 + n'_2} \phi_{n_1 0}(0) \phi_{n_2 0}(0) \phi_{n'_1 0}(0) \phi_{n'_2 0}(0) \delta_{l_1 0} \delta_{l'_1 0} \delta_{l_2 0} \delta_{l'_2 0} . \end{aligned} \quad (14)$$

B. Renormalization

Next we discuss the renormalization of the Hamiltonian, Eq. (2). For convenience, all energies are given in units of $\hbar\omega$. The coupling constants $g^{(2)}$ and $g^{(3)}$ depend on the regulator N . At each value of N , i.e. in each model space, their values have to be fixed by one two-body and one three-body observable. All other observables are then predictions.

As the two-body input parameter, we use an eigenenergy $E^{(2)}$ in the two-body spectrum with $L = 0$. Using the analytical solution derived by Busch and collaborators [14],

$$\frac{\beta}{a} = \sqrt{2} \frac{\Gamma(3/4 - E^{(2)}/2)}{\Gamma(1/4 - E^{(2)}/2)} , \quad (15)$$

this energy $E^{(2)}$ is directly related to the S-wave scattering length a .

The relation between $g^{(2)}$ and $E^{(2)}$ for a given N can be found analytically by exploiting of the separability of the interaction. We define

$$f_{n\epsilon} \equiv \begin{cases} \phi_{n0}(0) , & \text{for contact interactions,} \\ (1 + \epsilon^2)^{-3/2} \left(\frac{1 - \epsilon^2}{1 + \epsilon^2} \right)^n \phi_{n0}(0) , & \text{for smeared contact interactions.} \end{cases} \quad (16)$$

As discussed in Sec. II A, the matrix elements in the 2-body sector for $L = l = 0$ are given by

$$\langle n | H^{(2)} | n' \rangle = \left(2n + \frac{3}{2} \right) \delta_{n,n'} + g^{(2)} f_{n\epsilon} f_{n'\epsilon}. \quad (17)$$

In the model space corresponding to N , the solution $|\psi_{E^{(2)}}\rangle$ of the eigenvalue problem with the eigenvalue $E^{(2)}$ is expanded in oscillator functions

$$|\psi_{E^{(2)}}\rangle = \sum_{n=0}^{N/2} c_n^{E^{(2)}} |n\rangle. \quad (18)$$

Applying the Hamiltonian to Eq. (18) and projecting on the oscillator state $|k\rangle$, we obtain

$$\left(2k + \frac{3}{2} \right) c_k^{E^{(2)}} + \sum_{n=0}^{N/2} g^{(2)} f_{k\epsilon} f_{n\epsilon} c_n^{E^{(2)}} = E^{(2)} c_k^{E^{(2)}}. \quad (19)$$

Solving for $c_k^{E^{(2)}}$ and reinserting the result in Eq. (19), we find the running of the coupling constant $g^{(2)}$ with N :

$$\frac{1}{g^{(2)}(N)} = - \sum_{n=0}^{N/2} \frac{f_{n\epsilon}^2}{2n + \frac{3}{2} - E^{(2)}}. \quad (20)$$

The three-body coupling constant $g^{(3)}$ is fixed by an energy of the three-body system $E^{(3)}$. The solution $|\alpha_N\rangle$ of the three-body system without three-body interaction for a given value of N is:

$$|\alpha_N\rangle = \sum_{n_1 l_1, n_2 l_2, L} Z_N(\alpha_N; n_1 l_1, n_2 l_2, L) |n_1 l_1, n_2 l_2, L\rangle, \quad (21)$$

with energy eigenvalue $D_N(\alpha_N)$. Note that the eigenstates are degenerate in the total angular momentum projection M . With these states, we calculate the matrix elements for the complete Hamiltonian including the three-body interaction

$$\begin{aligned} \langle \alpha_N | H^{(3)} | \alpha'_N \rangle &= D_N(\alpha_N) \delta_{\alpha_N, \alpha'_N} \\ &+ g^{(3)}(N) \left(\sum_{n_1, n_2} Z_N(\alpha_N; n_1 0, n_2 0, 0) f_{n_1\epsilon} f_{n_2\epsilon} \right) \left(\sum_{n'_1, n'_2} Z_N(\alpha'_N; n'_1 0, n'_2 0, 0) f_{n'_1\epsilon} f_{n'_2\epsilon} \right). \end{aligned} \quad (22)$$

Requiring the energy of the state $|\alpha_N\rangle$ to be $E^{(3)}$ for all N , the renormalization condition for the three-body coupling follows:

$$\frac{1}{g^{(3)}(N)} = - \sum_{\alpha_N} \frac{\left(\sum_{n_1, n_2} Z_N(\alpha_N; n_1 0, n_2 0, 0) f_{n_1\epsilon} f_{n_2\epsilon} \right)^2}{D_N(\alpha_N) - E^{(3)}}. \quad (23)$$

Note that the expansion coefficients $Z_N(\alpha_N; n_1 0, n_2 0, 0)$ as well as the eigenvalue $D_N(\alpha_N)$ explicitly depend on N . The full spectrum in a model space for given N can then be determined with these coupling constants by diagonalization of the Hamiltonian matrix. Our general strategy for calculating the Hamiltonian matrix for a system of A identical bosons is described in Appendix A.

C. Running of $g^{(2)}$ and $g^{(3)}$

In this subsection, we study the running of the coupling constants $g^{(2)}$ and $g^{(3)}$ for contact interactions in detail. Stetcu et al. [28] rewrote the sum in Eq. (20) in terms of Γ -functions and the generalized hypergeometric function ${}_3F_2$. They found an explicit relation for $g^{(2)}(N)$ from which the behavior for large N can be obtained.

Here, we provide an alternative derivation of the behavior of $g^{(2)}(N)$ for large values of N using an integral representation of the sum in Eq. (20). For $E^{(2)} < 3/2$ each term in the sum is positive and the denominator grows monotonously. We examine the behavior for very large N . With the Euler-Maclaurin formula the sum can be approximated as an integral

$$-\frac{1}{g^{(2)}(N)} = \sum_{n=0}^{N/2} \frac{\phi_{n0}^2(0)}{2n + \frac{3}{2} - E^{(2)}} = \frac{1}{\pi^{3/2}} \int_1^{N/2} \frac{\Gamma(x + 3/2) dx}{\Gamma(3/2)\Gamma(x + 1)(2x + \frac{3}{2} - E^{(2)})} + \mathcal{O}(1), \quad (24)$$

where $\phi_{n0}(0)$ was substituted with Eq. (10). The quotient of Gamma functions can be expanded in x ,

$$\frac{\Gamma(x + 3/2)}{\Gamma(3/2)\Gamma(x + 1)} = \frac{1}{\Gamma(3/2)} \sqrt{x} + \mathcal{O}\left(\frac{1}{\sqrt{x}}\right). \quad (25)$$

Inserting this expansion in Eq. ((24)) and integrating, we find

$$g^{(2)}(N) = -\frac{\pi^2}{\sqrt{2}} \frac{1}{\sqrt{N}} + \mathcal{O}(1/N). \quad (26)$$

Thus the coupling constant vanishes as $1/\sqrt{N}$. Identifying \sqrt{N} with the momentum cutoff Λ , this is consistent with the renormalization in free space [3]. We thus expect the leading errors from finite N in our effective theory to scale with $1/\sqrt{N}$.

For $E^{(2)} < 3/2$, the coupling rapidly approaches zero as N is increased. In the case that $E^{(2)} > 3/2$, the terms in the sum in Eq. (24) are negative at first until $n > (E^{(2)}/2 - 3/4)$. The coupling $g^{(2)}(N)$ as a function of $N \in \mathbb{R}$ thus develops a minimum for $N \rightarrow (E^{(2)}/2 - 3/4)$ and has a pole as N is increased further. For even larger N it approaches zero as well.

For smeared contact interactions an additional damping factor appears. For Eq. (24), we have

$$\begin{aligned} -\frac{1}{g^{(2)}(N)} &= \frac{1}{(1 + \epsilon^2)^3} \sum_{n=0}^{N/2} \frac{\phi_{n0}^2(0)}{(2n + \frac{3}{2} - E^{(2)})} \left(\frac{1 - \epsilon^2}{1 + \epsilon^2}\right)^{2n} \\ &= \frac{1}{\pi^{3/2}(1 + \epsilon^2)^3} \int_0^{N/2} \frac{\Gamma(x + 3/2) dx}{\Gamma(3/2)\Gamma(x + 1)(2x + \frac{3}{2} - E^{(2)})} \left(\frac{1 - \epsilon^2}{1 + \epsilon^2}\right)^{2x} + \mathcal{O}(1). \quad (27) \end{aligned}$$

The integral now converges to a constant for $N \rightarrow \infty$ exponentially at a fixed value of ϵ . Thus, the coupling constant converges to a finite number. Note, that the larger ϵ is, the faster the coupling constant converges and the energy spectrum becomes independent of N . This result reflects the additional regularization of the contact interaction by the smearing.

In the inset of Fig. 2, we illustrate the behavior of the running coupling constant $\sqrt{N}g^{(2)}$ for $\epsilon = 0$. We show $\sqrt{N}g^{(2)}$ in the unitary limit for the renormalization energies $E^{(2)} = 0.5$

(ground state) and $E^{(2)} = 16.5$ (8th excited state). In the case of $E^{(2)} = 0.5$, the running coupling $\sqrt{N} g^{(2)}$ has already converged to a constant value for small values of N and shows no structure. For $E^{(2)} = 16.5$, the situation is as described above. The coupling constant approaches zero for N around 14 where the denominator of the right hand side of Eq. (24) changes sign. Moreover, it changes from large positive to large negative values around $N = 21$. This behavior can be understood by looking at the spectrum for $E^{(2)} = 16.5$ shown in Fig. 2. For small values of N , the model space is not large enough to describe the ground state adequately. The behavior of the coupling constant $\sqrt{N} g^{(2)}$ is exactly such that this new state enters the renormalized spectrum from minus infinity keeping the other states unchanged. In the continuum case, a similar behavior is observed for the three-body spectrum [3, 34]. For larger values of N , when the model space is large enough to describe the ground state, the running coupling $\sqrt{N} g^{(2)}$ approaches the same value for both cases.

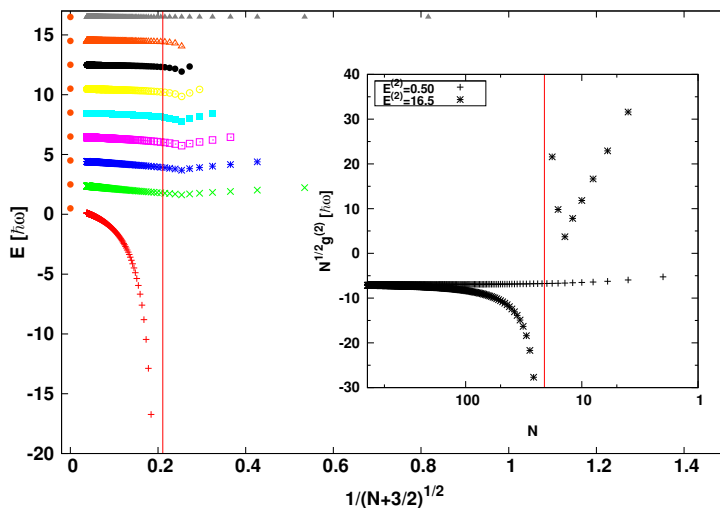


Figure 2. Energy spectrum in the two-body sector for $E^{(2)} = 16.5$. The dots on the left show the exact energies. The inset shows the running coupling constants $\sqrt{N} g^{(2)}$ in the unitary limit for renormalization energies $E^{(2)} = 0.5$ and $E^{(2)} = 16.5$.

For the coupling constant $g^{(3)}$ the situation is more complicated. The eigenvalues $D(\alpha)$ as well as the eigenstates now depend on the cutoff parameter N . Therefore it is not straightforward to derive the leading-order behavior of $g^{(3)}$ analytically. Werner et al. have provided a semi-analytic solution for the three-body problem in a harmonic trap in the unitary limit [16]. We use their results for the energy spectrum to benchmark our three-body calculations.

In the left panel of Fig. 3, we show the spectrum in the unitary limit for a three-body renormalization energy $E^{(3)} \approx 1.76$ as a function of N . At $N = 16$ a new three-body state enters the spectrum of the model space from minus infinity. For large N this state approaches the exact eigenenergy at -4 . In the inset, the corresponding coupling constant $g^{(3)}$ is shown. As in the two-body case, the coupling constant diverges, here around $N = 16$, and changes from large positive to large negative values. The three-body spectrum and the coupling constant in the continuum case show the same behavior [3]. The phenomena are the same as in the two-body case discussed above. In the right panel of Fig. 3, we present the energy spectra for the renormalization $E^{(3)} \approx 16.14$. This renormalization belongs to the energy spectrum in the full Hilbert space: $\dots, -5319.28, -10.29, 1.4, 3.68, 5.82, 7.92,$

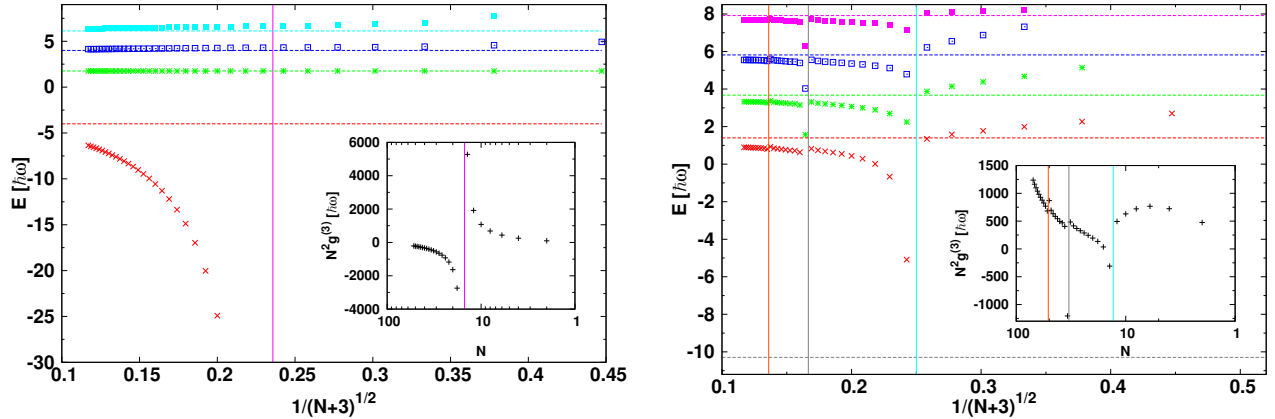


Figure 3. Left panel: Energy spectrum of Efimov-like states in the three-boson sector in the unitary limit ($E^{(2)} = 0.5$) for $E^{(3)} \approx 1.76$. The dashed lines indicate the exact energies [16]. Right panel: Energy spectrum for Efimov-like states in the unitary limit $E^{(2)} = 0.5$ with $E^{(3)} \approx 16.14$ for contact interactions. The running coupling constants $N^2 g^{(3)}$ corresponding to both cases are shown in the insets. Poles are indicated by vertical solid lines.

9.99, 12.05, 14.10, 16.14, \dots . The states with energies lower than 1.4 cannot be found inside the feasible model spaces for this renormalization energy. Remarkably, the states approach the exact energies but at specific values of the cutoff marked by vertical lines the spectrum rearranges. The smallest value of N corresponds to the appearance of a ground state at energy 1.4.

At the two largest cutoff values marked, there are small discontinuities in the energy. These discontinuities are artifacts of the renormalization method and do not correspond to new states entering the spectrum. Since we work in a finite model space, not only the Efimov-like states but also the universal states depend very weakly on the three-body interaction. In the special case when for a given cutoff \bar{N} the renormalization energy $E^{(3)}$ exactly coincides with the eigenvalue of a universal state corresponding to another spectrum with renormalization energy $\bar{E}^{(3)}$, our computer code erroneously renormalizes to the spectrum characterized by $\bar{E}^{(3)}$. The energy values in the neighborhood of such points should therefore be discarded.

In the inset of the right panel of Fig. 3, the behavior of the corresponding coupling constant is shown. The coupling constant has a salient behavior at three positions indicated by the vertical lines. At the smallest value of N where the ground state enters into the spectrum from below, the coupling changes from large positive to large negative values. The approximate pole which is expected at this position due to the discrete nature of the cutoff N is strongly distorted on the right wing due to finite cutoff effects. At the two larger values of N , there are discontinuities due to the renormalization artifacts discussed above. Moreover, for even larger N the coupling approaches an approximate pole corresponding to the addition of a new ground state at energy -10.29 . This pole is not reached in our calculation; it would require a larger N .

D. Error Analysis

There are various sources of errors in our calculation. In this subsection, we perform a detailed error analysis.

First, there are corrections due to the ultraviolet cutoff parameter N . Our considerations in subsection IIC showed that the finite model space also implies an infrared cutoff which vanishes as N is increased. The errors due to both cutoffs show the same scaling behavior in N . Therefore, we expect corrections in the energy eigenvalues of order $1/\sqrt{N + (A - 1)3/2}$ for large N . The shift of N by $(A - 1)3/2$ under the square root takes into account the zero-point energy of the free A -body system. We can extract the scaling behavior of these corrections from the error analysis introduced by Lepage [35]. In Fig. 4, we show the deviation of the lowest three-body energy eigenvalues from the exact values in the unitary limit $E^{(2)} = 0.5$ with three-body renormalization energy $E^{(3)} = -1$. The double-logarithmic plot shows a linear dependence of the energy differences on $\log(N + 3)$ for large N values. From a linear fit to the five largest values of N , we find a slope of $s \approx -0.6$ for the first four Efimov states above the state used for renormalization. The small difference to the expected value of $s = -0.5$ could be due to contamination from higher order corrections. As a consequence, the cutoff dependence for contact interactions is in agreement with power counting arguments based on identifying the continuum cutoff Λ with $1/\sqrt{N + (A - 1)3/2}$. A similar power law dependence of the leading corrections to three-body energies for contact interactions was observed by Furnstahl et al. [36].

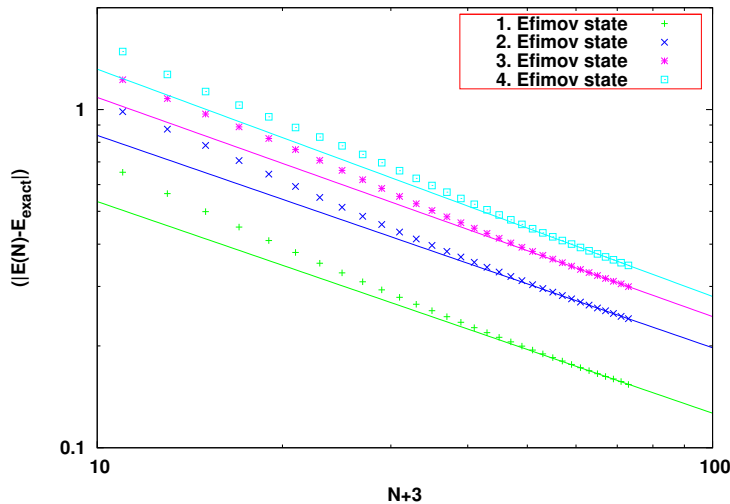


Figure 4. Corrections in energy eigenvalues as a function of $N + 3$ with $A = 3$, $E^{(2)} = 0.5$, $E^{(3)} = -1$.

In the case of smeared contact interactions, we find an exponential dependence on \sqrt{N} . In the two-body sector, we consider model spaces with cutoffs up to $N = 700$. In a Lepage plot of $\log(|E_N - E_\infty|)$ we find for large cutoffs a slope of about -0.5 . This implies that for large N the calculated energies behave as

$$E_N \approx E_\infty + c_1 e^{-c_2 \sqrt{N}}. \quad (28)$$

Thus the smearing changes the leading corrections from an inverse power law to an exponential behavior.

The convergence properties of variational calculations using basis expansions have been studied already in the 1970's [37, 38]. More recently, the convergence properties of ab initio calculations of light nuclei in a harmonic oscillator basis were investigated [33, 39]. Due to their singularity, we expect the contact interactions to behave quite differently, but it is interesting to compare our results for smeared interactions to Refs. [33, 39]. However, one has to keep in mind that we consider a physical trapping potential instead of a mere basis expansion. Moreover, in our calculation the effective interaction is renormalized at each N in order to keep the energies of a given two- and three-body state fixed.

Our results show the same exponential dependence on the ultraviolet cutoff and on the infrared cutoff $\lambda_{sc} \propto 1/\sqrt{N+3/2}$ as observed by Coon et al. for the Idaho N3LO potential [33]. Furnstahl et al. [39], in contrast, observed a Gaussian dependence on the UV cutoff

$$E_N \approx E_\infty + A_0 e^{-A_1(\sqrt{N})^2}, \quad (29)$$

using similarity renormalization group (SRG)-evolved chiral interactions, but their dependence on the infrared cutoff is consistent with ours. The difference might be due to the use of SRG-evolved interactions, but this question requires further study.

If we want to extract the energies for genuine contact interactions from smeared contact interactions, there are also errors due to the width parameter ϵ which generates a finite interaction range. The corresponding two-body problem in free space is separable and can be solved analytically. In our calculations, we determine the coupling constants from matching to energy levels in the oscillator. One two-body energy level $E^{(2)}$ is kept constant in each model space and the coupling constant $g^{(2)}$ is determined from this matching condition (cf. Eq. (20)). We find:

$$\begin{aligned} \frac{1}{g_N^{(2)}(\epsilon)} &= - \left((1 + \epsilon^2) \sqrt{\pi} \right)^{-3} \sum_{n=0}^{N/2} \frac{\left(\frac{1-\epsilon^2}{1+\epsilon^2} \right)^{2n} \frac{(2n+1)!!}{n! 2^n}}{2n + \frac{3}{2} - E^{(2)}}, \\ &\xrightarrow{N \rightarrow \infty} \left((1 + \epsilon^2) \sqrt{\pi} \right)^{-3} (2E^{(2)} - 3)^{-1} {}_2F_1 \left(\frac{3}{2}, \frac{3}{4} - \frac{E^{(2)}}{2}; \frac{7}{4} - \frac{E^{(2)}}{2}; \frac{(\epsilon^2 - 1)^2}{(\epsilon^2 + 1)^2} \right), \end{aligned} \quad (30)$$

where ${}_2F_1(a, b; c; z)$ denotes a hypergeometric function. The limit $N \rightarrow \infty$ yields the coupling constant in the full Hilbert space.

We use ϵ as a smearing parameter and are interested in the behavior for small ϵ . Expanding the first and second line of Eq. (30), we find:

$$g_\infty^{(2)}(\epsilon) = -2\pi^{\frac{3}{2}} \epsilon - \frac{4\pi^2 \Gamma(\frac{3}{4} - \frac{E^{(2)}}{2})}{\Gamma(\frac{1}{4} - \frac{E^{(2)}}{2})} \epsilon^2 - 2\pi^{\frac{3}{2}} \left(1 + 4E^{(2)} + \frac{4\pi \Gamma(\frac{3}{4} - \frac{E^{(2)}}{2})^2}{\Gamma(\frac{1}{4} - \frac{E^{(2)}}{2})^2} \right) \epsilon^3 + \mathcal{O}(\epsilon^4), \quad (31)$$

$$g_N^{(2)}(\epsilon) = c_0(N, E^{(2)}) + c_2(N, E^{(2)})\epsilon^2 + \mathcal{O}(\epsilon^4). \quad (32)$$

Remarkably, the results for finite and infinite N differ fundamentally since the limits $\epsilon \rightarrow 0$ and $N \rightarrow \infty$ do not commute. For $N \rightarrow \infty$, the coupling constant depends linearly on ϵ in leading order and vanishes for $\epsilon \rightarrow 0$. For finite N , the leading term is independent of ϵ and the first correction is of order ϵ^2 . The constant term in ϵ is a consequence of regularization with N but the vanishing of the correction linear in ϵ is unexpected. The expansion parameter $c_0(N, E^{(2)})$ vanishes like $1/\sqrt{N}$ for $N \rightarrow \infty$.

The corresponding two-body energies show a similar behavior. First, the value of $g^{(2)}$ is fixed for a given ϵ and $E^{(2)}$. The other energies $E_i^{(2)}$ can then be calculated numerically using a root-finding algorithm. For $N = \infty$ and small ϵ the energies $E_i^{(2)}(\epsilon, E^{(2)})$ depend linearly on ϵ . In order to extract the results for a zero-range contact interaction from a calculation with smeared interactions, a linear extrapolation in ϵ is thus appropriate. For finite N , however, the dependence of the excitation energies $E_i^{(2)}(\epsilon, E^{(2)}, N)$ on ϵ is different. For $\epsilon \rightarrow 0$, we find $|E_i^{(2)}(\epsilon, E^{(2)}, N) - E_i^{(2)}(0, E^{(2)}, N)| \propto \epsilon^2$ and an extrapolation in ϵ does not reproduce the result for a zero-range contact interaction. The ϵ -dependence of the energies is illustrated schematically in Fig. 5. In order to extract the contact interaction results from

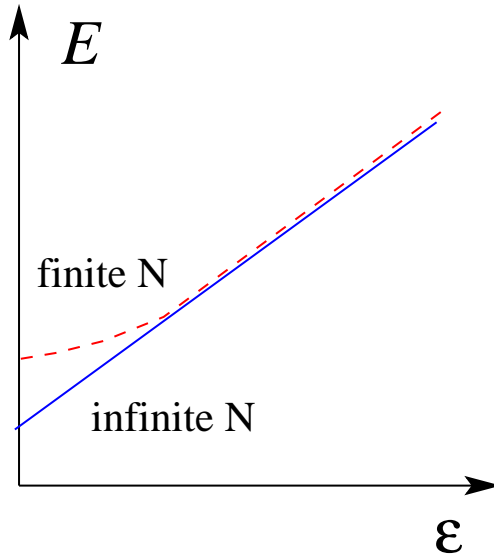


Figure 5. Schematic dependence of energies on the smearing parameter ϵ for finite N (dashed line) and infinite N (solid line).

smeared interactions, it is therefore important to extrapolate in N first (or use numerically converged values) and then extrapolate to $\epsilon = 0$ in a second step.

The variation of the energies with ϵ can be interpreted as a dependence on the effective range r_e of the two-body interaction. The effective range parameters in terms of the effective coupling constant $g^{(2)}$ in the continuum case are (See Appendix C):

$$\frac{1}{a} = \frac{\sqrt{2}\pi}{g^{(2)}} + \frac{1}{\sqrt{2\pi}\epsilon} \quad \text{and} \quad r_e = \frac{\sqrt{2}\epsilon}{\sqrt{\pi}} - \frac{\sqrt{8\pi}\epsilon^2}{g^{(2)}}. \quad (33)$$

These relations are valid in the full Hilbert space but not in the restricted model space characterized by finite N . Analog to the case without a trap, our numerical results and Eqs. (33) then imply that the leading corrections to the energies $E_i^{(2)}$ for contact interactions are linear in the effective range r_e .

We have also studied the ϵ -dependence in the three-body sector. In the left panel of Fig. 6, we show the corrections from finite ϵ for finite N . We plot the deviation of results for smeared interactions with $\epsilon \neq 0$ from contact-interactions results with $N = 70$. We pick out the unitary limit for contact interactions, which corresponds to $E^{(2)} = 0.5$. Please note, that we keep the two-body ground state constant while ϵ is changed. For finite ϵ , the system

is not exactly in the unitary limit anymore. For small ϵ there is a linear dependence in the double-logarithmic plot. The fit yields a slope round about $s = 2$ for the state presented, which implies a quadratic dependency of the corrections in ϵ for $\epsilon \rightarrow 0$ in agreement with the behavior in the 2-body sector.

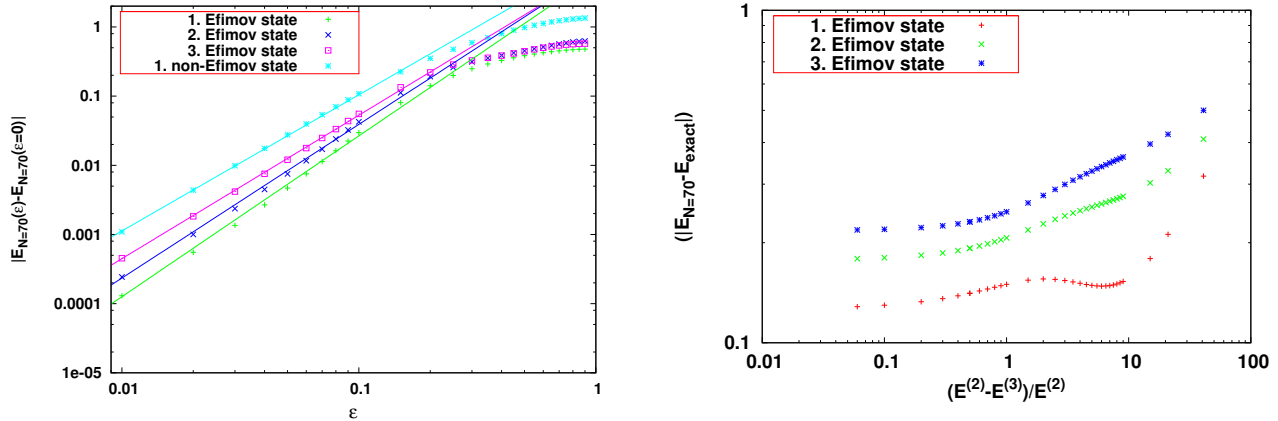


Figure 6. Left panel: Corrections in energy eigenvalues as a function of ϵ with $A = 3$, $E^{(2)} = 0.5$, $E^{(3)} = 0.5$. Right panel: Corrections in $(E^{(2)} - E^{(3)})/E^{(2)}$ for the unitary limit with $A = 3$.

Finally, there are corrections from a mismatch in renormalization energies $E^{(2)}$ and $E^{(3)}$. In an effective theory, only states with excitation energies small compared to the cutoff scale of the effective theory can be described. Clearly, the renormalization energies must be chosen in this energy range. For $E^{(2)} \neq E^{(3)}$, we expect errors governed by $(E^{(2)} - E^{(3)})$ from the mismatch in the renormalization energies. For contact interactions ($\epsilon = 0$), we have investigated the errors in $(E^{(2)} - E^{(3)})$ numerically. For this purpose, we chose the unitary limit and varied $E^{(3)}$. The right panel of Fig. 6 shows the deviation of the exact results from results in the model space for various $(E^{(2)} - E^{(3)})$. As expected, the corrections grow with increasing $|E^{(2)} - E^{(3)}|$. Thus in practice, it is desirable to choose $E^{(2)} \approx E^{(3)}$ to minimize this type of errors.

III. RESULTS

We will now use these insights to study the energy spectra of A -boson systems for $A = 3, 4, 5, 6$ in a trap. We will follow two strategies to obtain the spectra from numerical calculations:

1. use contact interactions and extrapolate in $1/\sqrt{N + (A - 1)3/2}$ as in our previous work [26], and
2. use smeared contact interactions and extrapolate the converged results in N linearly in the width parameter ϵ .

The difference between the two methods will be used to estimate the errors in our calculation.

A. Three identical bosons

At first, we consider the 3-boson sector. In the left panel of Fig. 7, the eigenvalues of the first excited $L^\pi = 0^+$ state are shown as a function of the cutoff parameter $N \leq 70$ for various smearing parameters ϵ in oscillator lengths β . The corresponding renormalization energies are $E^{(2)} = 0.5$ and $E^{(3)} = -1$. For small model spaces the results are identical

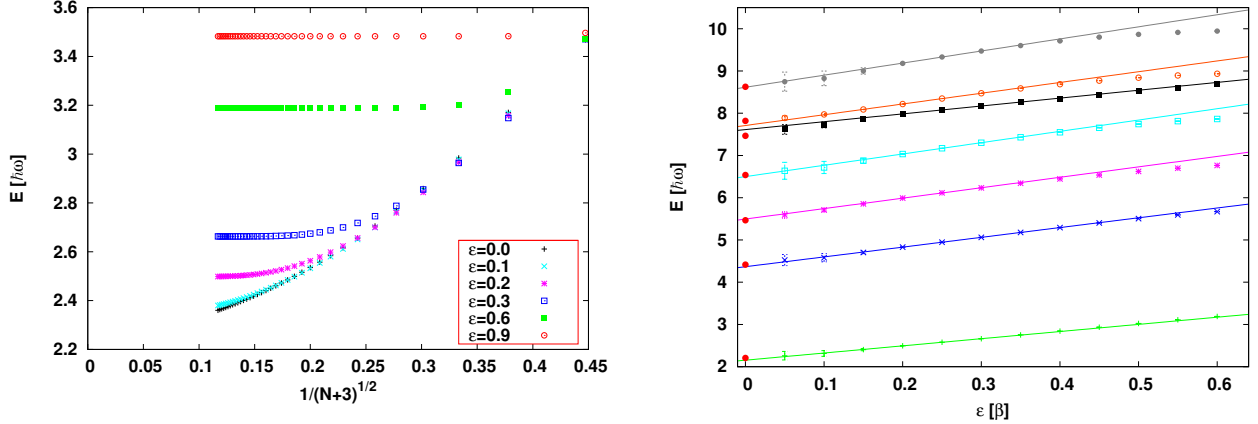


Figure 7. Left panel: Eigenvalue for the first excited $L^\pi = 0^+$ state with $A = 3$ as a function of N with $E^{(2)} = 0.5$ and $E^{(3)} = -1$ for various ϵ . Right panel: The converged eigenvalues as a function of ϵ . $L^\pi = 0^+$, $E^{(2)} = 0.5$ and $E^{(3)} = -1$. The points at $\epsilon = 0$ denote the exact eigenvalues from [16]. The dashed lines are linear fits to the values for $\epsilon \leq 0.3$ used to extrapolate to $\epsilon = 0$.

for all interaction widths. With increasing interaction width ϵ the eigenvalues converge for smaller values of N . The converged eigenvalues do not coincide with the results for contact interactions. However, as discussed in the previous section, the parameter ϵ can now be used as a extrapolation parameter instead of N .

The converged eigenvalues are given as a function of ϵ in the right panel of Fig. 7 for the 5 lowest $L^\pi = 0^+$ excited states. The solid lines are linear extrapolations of the data points for $\epsilon \leq 0.3$ and the results agree with the exact values known for contact interactions in the unitary limit [16] within 3% errors. The error bars of the data points are estimated by the difference of the eigenvalues related to the two highest cutoff parameters N , i.e. with these two eigenvalues the exact one is approximated by linear extrapolation and the error is estimated as the difference between the state with the highest cutoff parameter and the estimated one. In Fig. 7 the two model space sizes correspond to $N = 70$ and $N = 68$.

In Fig. 8, we show the spectra of Efimov-like states in the unitary limit ($E^{(2)} = 0.5$) for $E^{(3)} = 0.5$ and $E^{(3)} = -4$ in order to illustrate the significance of the mismatch in renormalization scales. With a linear extrapolation the exact values for $E^{(3)} = -4$ are undershot systematically. For larger $E^{(3)}$ the extrapolation in N achieves better results than a linear extrapolation in ϵ . Our method clearly has larger errors for $E^{(3)} = -4$.

Finally, we give in Fig. 9 a non-unitary example with $E^{(2)} = -2$. In the left panel the eigenvalues for the renormalization energy $E^{(3)} = -1$ are shown as a function of the width ϵ and in the right panel for $E^{(3)} = -5$. The results are linearly extrapolated like in the unitary limit. At $\epsilon = 0$ the results for contact interactions extrapolated with a quadratic polynomial in $1/\sqrt{N+3}$ are added. The uncertainties from the extrapolation are estimated conservatively as the energy shift from the last calculated eigenvalues to the extrapolated one.

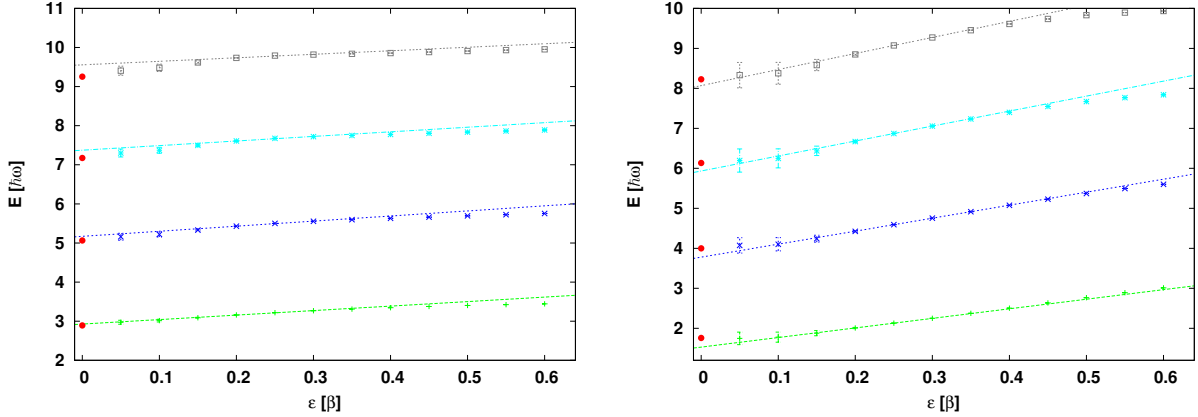


Figure 8. Spectrum of Efimov-like $L^\pi = 0^+$ states with $A = 3$ in the unitary limit as a function of ϵ . At $\epsilon = 0$ exact eigenenergies are drawn in. Left panel: Renormalization energy $E^{(3)} = 0.5$. Right panel: Renormalization energy $E^{(3)} = -4$.

Inside relative errors of 3.5% referred to the ground state with eigenenergy -5 respectively -1 both results coincide. Our method clearly has larger errors for $E^{(3)} = -5$.

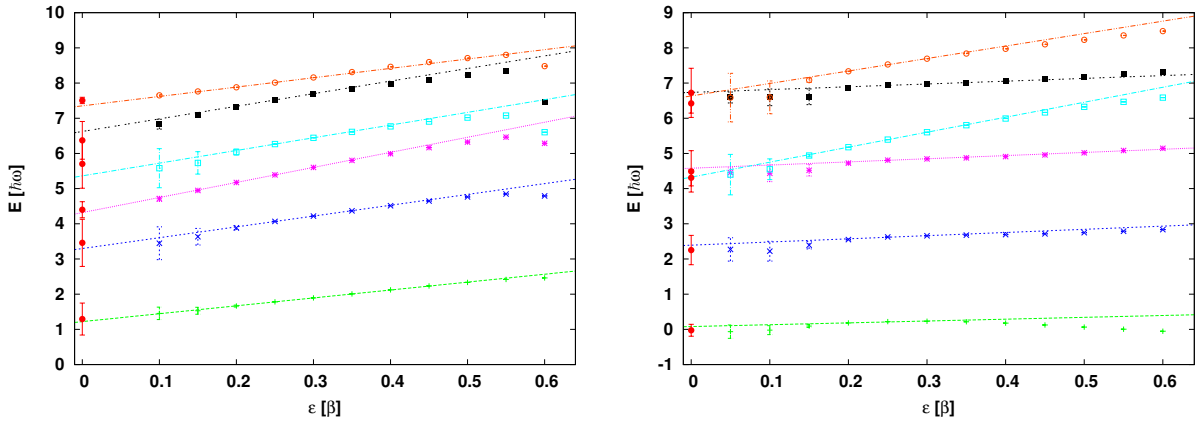


Figure 9. $L^\pi = 0^+$ eigenvalues for $A = 3$ as a function of ϵ with $E^{(2)} = -2$. The points at $\epsilon = 0$ denote the extrapolated results for contact interactions. The lines are linear extrapolations to $\epsilon = 0$. Left panel: $E^{(3)} = -1$ Right panel: $E^{(3)} = -5$

B. Four identical bosons

In Ref. [26], we published results for a 4-boson system with contact interactions. Here we revisit these calculations using smeared interactions. For instance, calculations for the unitary limit $E^{(2)} = 0.5$ with $E^{(3)} = -1$ with contact interactions $\epsilon = 0$ are compared to calculations with $\epsilon \neq 0$. We can reach cutoff values up to $N = 26$ which is significantly smaller than in the three-body sector. In Fig. 10, the eigenenergies for the ground and for the first excited states are shown for various model-space sizes. The solid lines are extrapolations with quadratic polynomials in $1/\sqrt{N + 9/2}$. As in the three-body sector the eigenvalues converge in N earlier for larger smearing parameters ϵ . However, for smeared

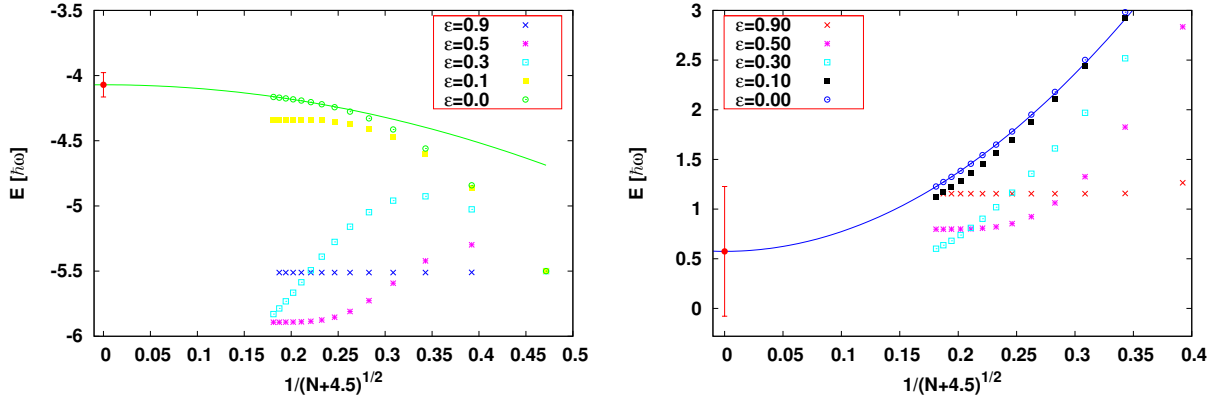


Figure 10. Four-boson $L^\pi = 0^+$ states with $E^{(2)} = 0.5$ and $E^{(3)} = -1$ for various smearing parameters ϵ as a function of $1/\sqrt{N+4.5}$. Left panel: Ground state. Right panel: First excited state. Solid lines are polynomial extrapolation.

interactions the eigenvalues of the ground state increase at first until they reach a maximum and begin to decrease afterwards. It is conceivable that for contact interactions and $\epsilon = 0.1$ the model spaces are too small in order to see the decrease of the eigenvalues. Thus, our extrapolation given in the left panel of Fig. 10 could have large systematic errors. Since contact interactions can behave quite differently from smeared interactions, however, a definite answer requires calculations at larger cutoffs N which are beyond the scope of this work. If the renormalization energies $E^{(2)}$ and $E^{(3)}$ are chosen equal, the non-monotonous behavior in ϵ does not appear. It becomes more severe as the mismatch between $E^{(2)}$ and $E^{(3)}$ is increased. The excited states do not show the non-monotonous behavior in ϵ at all. Their eigenvalues decrease monotonously with ϵ and for large ϵ they converge inside the model-space sizes considered here.

In Fig. 11 (left panel) we show the converged or extrapolated eigenvalues as a function of ϵ for the three lowest states with renormalization energies $E^{(2)} = 0.5$ and $E^{(3)} = -1$. In comparison to the three-body sector, we can diagonalize the Hamiltonian only in small model spaces (up to $N = 26$). Thus, just until $\epsilon = 0.35$ the eigenvalues have small error bars and we extrapolated the states linearly to $\epsilon = 0$. At $\epsilon = 0$ the eigenstates extrapolated via N with a quadratic polynomial in $1/\sqrt{N+9/2}$ and their estimated uncertainties are shown. For $\epsilon < 0.25$ the eigenvalues for the ground states cannot be determined with acceptable accuracy. The extrapolated results differ significantly and are at odds with each other for the ground state. This is due to the non-monotonic behavior of the ground state energy with ϵ discussed above. For the excited states this problem is not present and the results of the two extrapolations are compatible. In the right panel of Fig. 11, we show the results for $E^{(3)} = 0.5$. Since $E^{(2)} = E^{(3)}$, one expects less uncertainties for a fixed ϵ than for the case $E^{(2)} \neq E^{(3)}$ (see section IID). In particular, the ground state energies show no non-monotonous dependence on ϵ and the extrapolations in ϵ and N are consistent.

C. 5 and 6 identical bosons

We now apply our combined extrapolation technique to perform exploratory calculations of the spectra of 5 and 6 identical bosons. In order to keep the uncertainties as small as

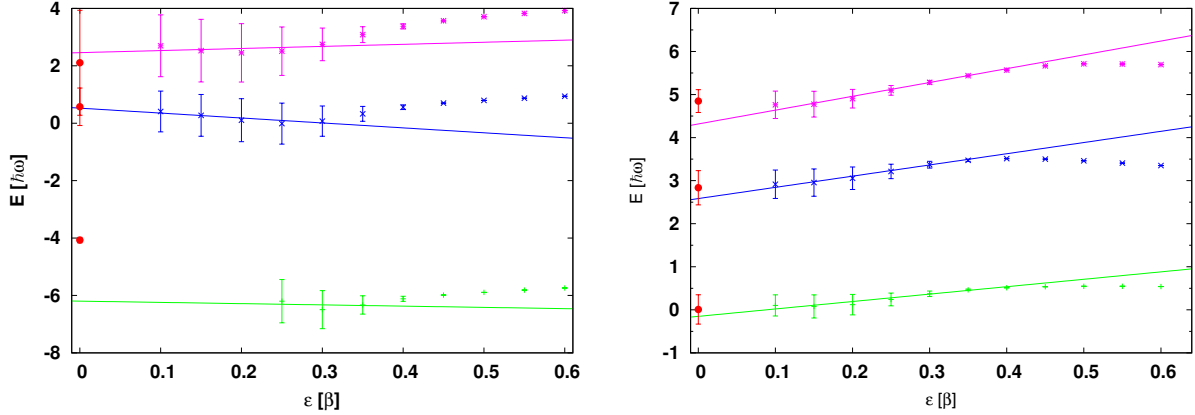


Figure 11. Lowest three energy states $L^\pi = 0^+$ for $E^{(2)} = 0.5$ as a function of ϵ for $A = 4$. Left panel: $E^{(3)} = -1$. Right panel: $E^{(3)} = 0.5$. The eigenvalues are linearly extrapolated. At $\epsilon = 0$ extrapolated eigenvalues for contact interactions drawn in.

possible, the renormalisations energies are chosen to be identical, i.e. $E^{(2)} = E^{(3)} = 0.5$. In particular, this removes the problem of the non-monotonous behavior of the energies as a function of ϵ discussed above for the four-body system. The cutoff parameter is $N = 20$ for 5 bosons and $N = 16$ for 6 bosons.

Our results for the three lowest energy $L^\pi = 0^+$ states with different smearing parameters ϵ are shown in Fig. 12. Due to the small model spaces, the uncertainties are significantly larger than for three and four bosons. The eigenenergies for contact interactions are extrapolated in N with a polynomial of second order in $1/\sqrt{N + (A - 1)/2}$. They are shown at $\epsilon = 0$ with conservative error bands. These approximated eigenvalues are consistent with extrapolations in ϵ for smeared contact interactions inside the error bands. Thus we conclude

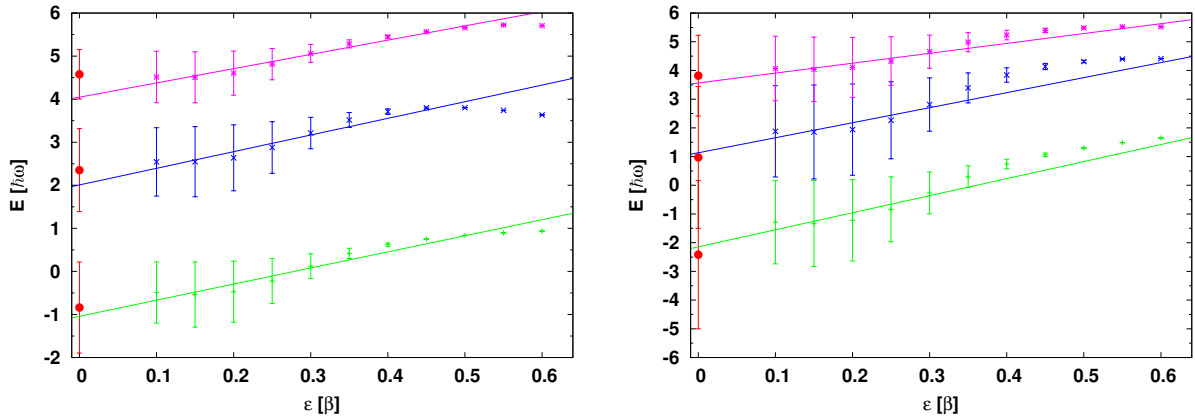


Figure 12. Lowest three energy states $L^\pi = 0^+$ for $E^{(2)} = 0.5$, $E^{(3)} = 0.5$ as a function of ϵ . Left panel: $A = 5$ ($N = 20$). Right panel: $A = 6$ ($N = 16$). The solid lines are linear extrapolations in ϵ . At $\epsilon = 0$ the eigenvalues extrapolated with a polynomial of second order in $1/\sqrt{N + (A - 1)/2}$ for contact interactions drawn in.

that the combined extrapolation in N and ϵ makes calculations in 5- and 6-boson systems with moderate computational resources possible.

In Table I, we have collected the extracted energies of the lowest three Efimov-like states

for the unitary limit ($E^{(2)} = 0.5$) and a three-body ground state energy fixed to $E^{(3)} = 0.5$ (cf. Figs. 8, 11, and 12). The numbers in the first two columns are the exact values for $A = 2$

$A = 2$	$A = 3$	$A = 4$	$A = 5$	$A = 6$
0.5	0.5	-0.1(2)	-0.9(2)	-2.3(3)
2.5	2.9	2.7(3)	2.2(3)	1.1(2)
4.5	5.1	4.6(5)	4.3(5)	3.7(3)

Table I. Energies of the three lowest Efimov-like states in systems with $A = 3, 4, 5, 6$ for the renormalization energies $E^{(2)} = 0.5$ corresponding to the unitary limit and $E^{(3)} = 0.5$. The column labeled $A = 2$ contains the three lowest two-body states. All energies are in units of $\hbar\omega$.

and $A = 3$ rounded to two digits of accuracy. The values for the columns labeled $A = 4$, $A = 5$, and $A = 6$ are extracted from our calculations. Here the number in parentheses gives the difference in the last digit between the extrapolation in N and ϵ which can serve as an estimate of the numerical error. The spectra are much more compressed than the corresponding free space results [4–9]. However, a similar pattern can be observed: starting from $A = 3$, every A -body state is accompanied by a corresponding $A + 1$ -body state. A second $A + 1$ -body state attached to the A -body state is not present in our calculation. It would be interesting to study the spectra also away from the unitary limit for fixed $E^{(3)}$ to investigate their systematics. However, due to the additional errors from the mismatch in $E^{(2)}$ and $E^{(3)}$ this is numerically more challenging.

IV. CONCLUSION AND OUTLOOK

In this paper, we have extended our previous work on universal few-body physics in harmonic confinement [26]. We investigated A -body systems with up to six particles using genuine and smeared contact interactions at leading order in the large scattering length.

The effective theory is defined within a finite model space with a cutoff N on the basis functions. We perform a detailed study of the running of the effective two- and three-body coupling constants $g^{(2)}$ and $g^{(3)}$ with N for contact interactions. In the two-body sector, the results of Stetcu et al. [28] for the running of $g^{(2)}$ are confirmed. For $g^{(3)}$, the limit cycle behavior expected from free space is observed and one complete cycle is traced numerically.

Moreover, we have performed a detailed analysis of the leading effective theory errors using Lepage plots. Our cutoff N on the size of the model space implies both an infrared cutoff of order $\sqrt{N + (A - 1)3/2}$ and an ultraviolet cutoff of order $1/\sqrt{N + (A - 1)3/2}$ in the effective theory. The errors in the eigenenergies from these cutoffs for genuine contact interactions scale as $1/\sqrt{N + (A - 1)3/2}$ in agreement with the expectations from the continuum case [3]. For smeared contact interactions, we find an exponential dependence on \sqrt{N} (cf. Eq. (28)) in agreement with Ref. [33].

An additional error is introduced if there is a mismatch in renormalization energies $E^{(2)}$ and $E^{(3)}$. We investigate these errors for contact interactions numerically and find that they are governed by the difference ($E^{(2)} - E^{(3)}$). To improve convergence $E^{(2)}$ and $E^{(3)}$ should be chosen as close as possible.

Smearing the contact interactions over distances of order ϵ improves the convergence with N considerably. Obviously, this smearing changes the interaction. In order to extract results for genuine contact interactions from calculations with finite ϵ , extrapolations in ϵ

are required. These extrapolations show a qualitatively different behavior for finite N and infinite N since the limits $N \rightarrow \infty$ and $\epsilon \rightarrow 0$ do not commute.

Based on our findings, the optimal strategy to extract the universal energies for contact interactions from numerical calculations in a finite model space when convergence can not be reached is to (i) use genuine contact interactions and extrapolate to $N = \infty$ and (ii) use converged energies for smeared contact interactions and extrapolate linearly to $\epsilon = 0$. The difference between the two methods can be used to estimate the errors in the calculation.

We use this strategy to calculate the spectra for A -boson systems with up to six bodies and study the case $E^{(2)} = E^{(3)} = 0.5$ in detail. We find that starting from $A = 3$, every A -body state is accompanied by a corresponding $A + 1$ -body state. A second $A + 1$ -body state is not observed. The combined extrapolation in N and ϵ makes the calculations possible with moderate computational resources and provides a first step towards calculating trapped many-body systems with resonant interactions. On the experimental side, the deterministic preparation of tunable few-fermion systems of up to ten particles in a microtrap was recently achieved by Serwane et al. [40]. Similar experimental studies of few-boson systems appear also promising.

If there is a mismatch in $E^{(2)}$ and $E^{(3)}$, the ground state energies for four and more particles show a non-monotonous dependence on N such that reliable results can only be obtained in large model spaces. For the excited states this problem is not present. In the future, it would be interesting to get a better analytical understanding of these corrections and possibly develop an renormalization group improved matching procedure for this case.

Finally, it would also be interesting to remove the trapping potential from the Hamiltonian (2) and apply our method to universal bound states in free space. For nuclear systems in the framework of the no-core shell model such a strategy was applied by Stetcu and collaborators [23].

ACKNOWLEDGMENTS

We thank S. Coon, R. Furnstahl, and U. van Kolck for discussions and S. Coon for pointing out previous work on the convergence properties of truncated basis expansions. This research was supported in part by the BMBF under contract No. 06BN7008. H.W.H. acknowledges the INT program ‘‘Light nuclei from first principles’’ during which this work was finalized.

Appendix A: Construction of the Hamiltonian Matrix

In this appendix, we discuss the construction of the Hamiltonian matrix for spinless bosonic wave functions, i.e. symmetric functions under transposition of the bodies. A symmetric basis for the model space of A bodies is constructed iteratively starting from the symmetric basis for two bodies.

a. Symmetric basis

To construct unnormalised symmetric states we define $P^{(2)} = (1 + T_{12})$ with the transposition T_{ik} between body i and k . With the oscillator states ϕ_{nlm} and the multi-index u we

thus have for 2 particles

$$P^{(2)}\phi_{nlm}(\vec{s}_1) = \phi_{nlm}(\vec{s}_1) + \phi_{nlm}(-\vec{s}_1) = \begin{cases} 0 & \text{for } l \text{ odd,} \\ 2\phi_{nlm}(\vec{s}_1) & \text{for } l \text{ even,} \end{cases} =: \widetilde{\phi^{(2)}}_u(\vec{s}_1). \quad (\text{A1})$$

The orthonormal basis for 2 particles with multi-index α thus is

$$\overline{\phi^{(2)}}_\alpha(\vec{s}_1) = \phi_{nlm}(\vec{s}_1) \quad \text{for } l \text{ odd.} \quad (\text{A2})$$

From these states coupled mixed-symmetric 3-body states are constructed as $[\overline{\phi^{(2)}}_\alpha \otimes \phi_{nl}]_M^L$. Since $[H, \vec{L}] = 0$, the matrix elements are independent of M and this quantum number is suppressed.

Accordingly, on the symmetric, unnormalised A -particle states we have

$$P^{(A)} = (1 + T_{1A} + \cdots + T_{(A-1)A})P^{(A-1)} = (1 + \sum_{i=1}^{A-2} T_{(A-1)i}T_{(A-1)A}T_{i(A-1)} + T_{(A-1)A})P^{(A-1)}.$$

Furthermore, we introduce the transformation matrix

$$C_{\text{sym}}^{(A-1) \rightarrow A}[z; \alpha', n'_2, l'_2, L'] = \langle [\overline{\phi^{(A-1)}}_{\alpha'} \otimes \phi_{n'_2 l'_2}]^{L'} | [\widetilde{\phi^{(A)}}_z] \rangle, \quad (\text{A3})$$

with multi-indices α' and z from the mixed-symmetric A -body states $[\overline{\phi^{(A-1)}}_{\alpha'} \otimes \phi_{n'_2 l'_2}]^{L'}$ to the symmetric A -body states $\widetilde{\phi^{(A)}}_z$, given by

$$\begin{aligned} C_{\text{sym}}^{(A-1) \rightarrow A}[z; \alpha', n'_2, l'_2, L'] &= \langle [\overline{\phi^{(A-1)}}_{\alpha'} \otimes \phi_{n'_2 l'_2}]^{L'} | P^{(A)} | [\overline{\phi^{(A-1)}}_\alpha \otimes \phi_{n_2 l_2}]^L \rangle, \quad (\text{A4}) \\ &= \langle [\overline{\phi^{(A-1)}}_{\alpha'} \otimes \phi_{n'_2 l'_2}]^{L'} | (1 + (A-1)T_{(A-1)A}) | [\overline{\phi^{(A-1)}}_\alpha \otimes \phi_{n_2 l_2}]^L \rangle, \quad (\text{A5}) \end{aligned}$$

where $z = \{\alpha, n_2, l_2, L\}$.

Our goal is to construct an orthonormal basis of symmetric A -body states $\overline{\phi^{(A)}}_\omega$. By diagonalization of the symmetric norm matrix

$$\mathcal{N}[z'; z] = \langle \widetilde{\phi^{(A)}}_{z'} | \widetilde{\phi^{(A)}}_z \rangle, \quad (\text{A6})$$

the diagonal matrix D of non-negative eigenvalues is found:

$$D = O \cdot \mathcal{N} \cdot O^T. \quad (\text{A7})$$

Vanishing eigenvalues do not correspond to symmetric states and respective eigenstates are eliminated. Thus, we find the non-quadratic transformation matrix B_{sym} from mixed-symmetric A -body states to orthonormal symmetric states:

$$B_{\text{sym}}^{(A-1) \rightarrow A}[\omega; \alpha', n'_2, l'_2 L'] = \frac{1}{\sqrt{D[\omega; j]}} O[j; z] A_{\text{sym}}^{(A-1) \rightarrow A}[z; n'_2, l'_2 L'], \quad (\text{A8})$$

where a sum over j and z is implied. Accordingly, the orthonormal basis of symmetric states is given by

$$|\overline{\phi^{(A)}}_\omega\rangle = B_{\text{sym}}^{(A-1) \rightarrow A}[\omega; \alpha, n_2, l_2, L] | [\overline{\phi^{(A-1)}}_\alpha \otimes \phi_{n_2 l_2}]^L \rangle. \quad (\text{A9})$$

b. *Explicit calculation of $C_{\text{sym}}^{(A-1)\rightarrow A}$*

The explicit calculation of $C_{\text{sym}}^{(A-1)\rightarrow A}$ is based on the Talmi-Moshinsky-transformation and on a change in the coupling scheme. With the operator $B_{\text{sym}}^{(A-2)\rightarrow(A-1)}$ Eq. (A5) yields

$$C_{\text{sym}}^{(A-1)\rightarrow A}[\alpha, n_2, l_2, L; \alpha', n'_2, l'_2, L'] = B_{\text{sym}}^{(A-2)\rightarrow(A-1)}[\alpha; \gamma, n_1, l_1, L_\alpha] B_{\text{sym}}^{(A-2)\rightarrow(A-1)}[\alpha'; \gamma', n'_1, l'_1, L'_{\alpha'}] \langle [[\overline{\phi^{(A-2)}}_{\gamma'}]^{L_{\gamma'}} \otimes \phi_{n'_1, l'_1}^{L'_{\alpha'}} \otimes \phi_{n_2, l_2}^{L'}]^{L'} | (1 + (A-1)T_{(A-1)A}) | [[\overline{\phi^{(A-2)}}_{\gamma}]^{L_\gamma} \otimes \phi_{n_1, l_1}^{L_\alpha} \otimes \phi_{n_2, l_2}^L] \rangle. \quad (\text{A10})$$

In order to calculate matrix elements of the operator $T_{(A-1)A}$, a transformation to coordinates $\vec{\lambda}$ and $\vec{\mu}$ is performed since $T_{(A-1)A}$ is diagonal in $\vec{\lambda}$ and $\vec{\mu}$ (see Fig. 13):

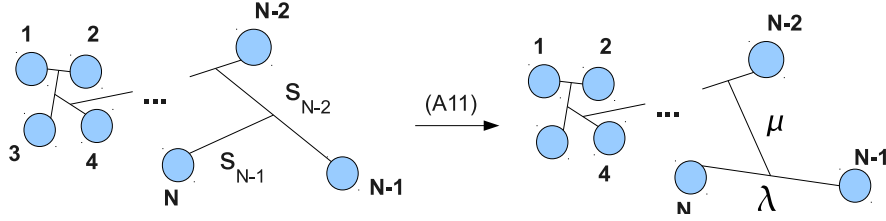


Figure 13. Talmi transformation from coordinates $\vec{s}_{(A-1)}$ and $\vec{s}_{(A-2)}$ to coordinates $\vec{\lambda}$ and $\vec{\mu}$

$$\begin{pmatrix} -\vec{\lambda} \\ \vec{\mu} \end{pmatrix} = \begin{pmatrix} \sqrt{\frac{A-2}{2(A-1)}} & -\sqrt{\frac{A}{2(A-1)}} \\ \sqrt{\frac{A}{2(A-1)}} & \sqrt{\frac{A-2}{2(A-1)}} \end{pmatrix} \cdot \begin{pmatrix} \vec{s}_{(A-2)} \\ \vec{s}_{(A-1)} \end{pmatrix}. \quad (\text{A11})$$

For this purpose the coupling scheme is changed by means of Wigner's 6j symbols [41] and in the new coupling scheme the Talmi-Moshinsky-transformation is exploited.

With the Brody-Moshinsky-brackets $\langle n_\lambda l_\lambda, n_\mu l_\mu; L_{12} | n_1 l_1, n_2 l_2 \rangle_{\frac{A}{A-2}}$ we find for the wave functions in terms of the coordinates $\vec{\lambda}$ and $\vec{\mu}$

$$\begin{aligned} & \left[[\overline{\phi^{(A-2)}}_{\gamma}]^{L_\gamma} \otimes \phi_{n_1, l_1}(\vec{s}_{(A-2)}) \right]^{L_\alpha} \otimes \phi_{n_2, l_2}(\vec{s}_{(A-1)}) \Big]^L = \\ & \sum_{L_{12}} (-1)^{L_\gamma + l_1 + l_2 + L} \sqrt{(2L_{12} + 1)(2L_\alpha + 1)} \begin{Bmatrix} L_\gamma & l_1 & L_\alpha \\ l_2 & L & L_{12} \end{Bmatrix} \\ & \sum_{\substack{l_\lambda, n_\lambda \\ l_\mu, n_\mu}} (-1)^{l_\lambda} \langle n_\lambda l_\lambda, n_\mu l_\mu; L_{12} | n_1 l_1, n_2 l_2 \rangle_{\frac{A}{A-2}} \left[\overline{\phi^{(A-2)}}_{\gamma} \right]^{L_\gamma} \otimes [\phi_{n_\lambda l_\lambda}(\vec{\lambda}) \otimes \phi_{n_\mu l_\mu}(\vec{\mu})]^{L_{12}} \Big]^L. \quad (\text{A12}) \end{aligned}$$

c. *Contributions of the 2- and 3- body contact interactions*

In addition to the matrix C_{sym} , also the 2-body interactions can be calculated in the coordinates $\vec{\lambda}$ and $\vec{\mu}$ introduced in the last section (see Fig. 13). Note that the contributions

of all 2-body interactions are equal since the bodies are identical. The 2-body interaction between body $(A - 1)$ and A depends only on the distance between these, which is proportional to $\vec{\lambda}$ and therefore the interaction is proportional to $\delta^{(3)}(\vec{\lambda})$. With combinatorics the number of interactions are determined: There are $\binom{A}{2} = \frac{A(A-1)}{2}$ two-body interactions.

Using the recoupling and the Talmi-Moshinsky-transformation one more time the contributions of all $\binom{A}{3} = \frac{A(A-1)(A-2)}{6}$ three-body interaction are determined in a similar fashion: For states expressed in terms of the coordinates $\vec{\nu}$, $\vec{\kappa}$ and $\vec{\lambda}$ the interactions can be readily calculated (see Fig. 14). The corresponding transformation is

$$\begin{pmatrix} \vec{\nu} \\ \vec{\kappa} \end{pmatrix} = \begin{pmatrix} \sqrt{\frac{A}{3(A-2)}} & -\sqrt{\frac{2(A-3)}{3(A-2)}} \\ \sqrt{\frac{2(A-3)}{3(A-2)}} & \sqrt{\frac{A}{3(A-2)}} \end{pmatrix} \cdot \begin{pmatrix} \vec{s}_{(A-3)} \\ -\vec{\mu} \end{pmatrix}. \quad (\text{A13})$$

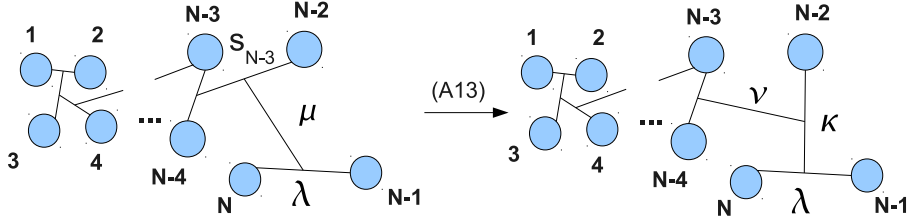


Figure 14. Talmi transformation from coordinates $\vec{s}_{(A-3)}$ and $\vec{\mu}$ to coordinates $\vec{\nu}$ and $\vec{\kappa}$

Appendix B: Smearing contact interaction

In this section we give the derivation for the matrix elements

$$\langle n_1 l_1 | V_G | n'_1 l'_1 \rangle = \frac{1}{(1 + \epsilon^2)^3} \phi_{n_1 0}(0) \left(\frac{1 - \epsilon^2}{1 + \epsilon^2} \right)^{n_1} \phi_{n'_1 0}(0) \left(\frac{1 - \epsilon^2}{1 + \epsilon^2} \right)^{n'_1} \delta_{l_1 0} \delta_{l'_1 0}. \quad (\text{B1})$$

For the interaction

$$\langle \vec{s} | V_G | \vec{s}' \rangle = \frac{1}{(2\pi\epsilon^2)^3} e^{-\frac{s^2}{2\epsilon^2}} e^{-\frac{s'^2}{2\epsilon^2}}, \quad (\text{B2})$$

we have

$$\langle n_1 l_1 | V_G | n'_1 l'_1 \rangle = \frac{1}{(2\pi\epsilon^2)^3} \int d^3 s \phi_{nl}(\vec{s}) e^{-\frac{s^2}{2\epsilon^2}} \int d^3 s' \phi_{n'l'}(\vec{s}') e^{-\frac{s'^2}{2\epsilon^2}}. \quad (\text{B3})$$

Moreover,

$$\int d^3 s \phi_{nl}(\vec{s}) e^{-\frac{s^2}{2\epsilon^2}} = \sqrt{4\pi} \int_0^\infty dr r^2 e^{-\frac{r^2}{2\epsilon^2}} R_{n0}(r) = N_{n0} \int_0^\infty dr r^2 e^{-\frac{1}{2}(1+\frac{1}{\epsilon^2})r^2} L_n^{(\frac{1}{2})}(r^2), \quad (\text{B4})$$

with the associated Laguerre polynomials $L_n^{(\frac{1}{2})}$ and the normalization $N_{n0} = \sqrt{\frac{1}{\sqrt{4\pi}} \frac{2^{n+3}n!}{(2n+1)!!}}$. By the substitution of $r^2 = x$ and with $\rho^2 = \frac{1}{2}(1 + \frac{1}{\epsilon^2})$, we get with the expansion of the Laguerre polynomials in monomials

$$\int d^3s \phi_{nl}(\vec{s}) e^{-\frac{s^2}{2\epsilon^2}} = \frac{\sqrt{4\pi}N_{n0}}{2} \sum_{i=0}^n \frac{(-1)^i}{i!} \frac{\Gamma(n + \frac{3}{2})}{\Gamma(i + \frac{3}{2})\Gamma(n - i + 1)} \int_0^\infty dx x^{\frac{1}{2}+i} e^{-\rho^2 x} \quad (\text{B5})$$

$$= \frac{\sqrt{4\pi}N_{n0}}{2} \sum_{i=0}^n \frac{(-1)^i}{i!} \frac{\Gamma(n + \frac{3}{2})}{\Gamma(n - i + 1)} \frac{1}{\rho^{3+2i}} \quad (\text{B6})$$

$$= \frac{\sqrt{4\pi}N_{n0}\Gamma(n + \frac{3}{2})}{2\rho^3} \frac{1}{n!} \sum_{i=0}^n \binom{n}{i} (-\rho^{-2})^i \quad (\text{B7})$$

$$= \frac{\sqrt{4\pi}N_{n0}(2n+1)!!}{2^{n+2}n!\rho^{2n+3}} (\rho^2 - 1)^n \sqrt{\pi}, \quad (\text{B8})$$

and replacing ρ and N_{n0} , we find

$$\langle n_1 l_1 | V_G | n'_1 l'_1 \rangle = \frac{1}{(1 + \epsilon^2)^3 \pi^{\frac{3}{2}}} \sqrt{\frac{(2n_1 + 1)!!}{n_1! 2^{n_1}}} \sqrt{\frac{(2n'_1 + 1)!!}{n'_1! 2^{n'_1}}} \left(\frac{1 - \epsilon^2}{1 + \epsilon^2}\right)^{n_1} \left(\frac{1 - \epsilon^2}{1 + \epsilon^2}\right)^{n'_1} \quad (\text{B9})$$

$$= \frac{1}{(1 + \epsilon^2)^3} \phi_{n_1 0}(0) \left(\frac{1 - \epsilon^2}{1 + \epsilon^2}\right)^{n_1} \phi_{n'_1 0}(0) \left(\frac{1 - \epsilon^2}{1 + \epsilon^2}\right)^{n'_1} \delta_{l_1 0} \delta_{l'_1 0}. \quad (\text{B10})$$

Appendix C: Effective range expansion for smeared contact interactions

For separable potentials

$$\langle \vec{s} | V | \vec{s}' \rangle = g^{(2)} \omega(\vec{s}) \omega(\vec{s}'), \quad (\text{C1})$$

we get for the T-matrix

$$\langle \vec{p} | T(z) | \vec{p}' \rangle = \left(\frac{1}{g^{(2)}} - B(z) \right)^{-1} v(\vec{p}) v(\vec{p}') \quad \text{with} \quad B(z) := \int \frac{d^3q}{(2\pi)^3} \frac{|v(\vec{q})|^2}{z - \frac{q^2}{2}} \quad (\text{C2})$$

from the Lippmann-Schwinger equation

$$T(z) = V + V(z - H_o)^{-1} T(z). \quad (\text{C3})$$

Here, $v(\vec{p})$ denotes the Fourier transform of $\omega(\vec{s})$

$$v(\vec{p}) = \int d^3s e^{i\vec{p}\vec{s}} \omega(\vec{s}). \quad (\text{C4})$$

For separable central potentials there is only s-wave scattering and we find for the scattering amplitude $f_0(p)$ with the effective range expansion

$$f_0(p) = \frac{1}{-\frac{1}{a} + \frac{1}{2}rp^2 + \mathcal{O}(p^4) - ip} \quad (\text{C5})$$

$$= -\frac{1}{2\pi} \lim_{\Delta \rightarrow 0} \langle \vec{p} | T(p^2/2 + i\Delta) | \vec{p}' \rangle \quad (\text{C6})$$

$$= [-2\pi |v(p)|^{-2} (1/g^{(2)} - B(p^2/2 + i\Delta))]^{-1}. \quad (\text{C7})$$

For the smeared contact interaction we have

$$\omega(\vec{s}) = \frac{1}{(2\pi\epsilon^2)^{\frac{3}{2}}} e^{-\frac{s^2}{2\epsilon^2}}, \quad v(\vec{p}) = e^{-\frac{p^2\epsilon^2}{2}}, \quad (\text{C8})$$

$$B(p^2/2 + i\Delta) = \frac{1}{\pi^2} \int_0^\infty dq \frac{q^2 e^{-\epsilon^2 q^2}}{p^2 - q^2 + i\Delta} = \frac{1}{2\pi^2} \int_0^\infty dk \frac{\sqrt{k} e^{-\epsilon^2 k}}{p^2 - k + i\Delta},$$

and the imaginary part of the denominator in $f_0(p)$ can be calculated with

$$\lim_{\Delta \rightarrow 0^+} \int_a^b dx \frac{f(x)}{x \pm i\Delta} = \mp i\pi f(0) + \mathcal{P} \int_a^b dx \frac{f(x)}{x}. \quad (\text{C9})$$

It follows for the imaginary part

$$\Im \frac{1}{f_0} = -\pi 2\pi e^{+\epsilon^2 p^2} \frac{1}{2\pi^2} p e^{-\epsilon^2 p^2} = -p \quad (\text{C10})$$

and for the real part

$$\Re \frac{1}{f_0} = \left[-\frac{2\pi}{g^{(2)}} - \frac{1}{\pi} \underbrace{\left[\mathcal{P} \int_{-\infty}^{+\infty} dq \frac{q^2 e^{-\epsilon^2 q^2}}{q^2 - p^2} \right]}_{A(p^2)} \right] e^{\epsilon^2 p^2}. \quad (\text{C11})$$

Moreover, it can be shown, that

$$A(p^2) = \sqrt{\pi} \frac{1 - 2\epsilon p \text{F}(\epsilon p)}{\epsilon}, \quad (\text{C12})$$

where the Dawson function is defined by

$$\text{F}(x) = e^{-x^2} \int_0^x dy e^{y^2} = x - \frac{2}{3}x^3 + \mathcal{O}(x^5). \quad (\text{C13})$$

The function $A(p^2)$ as well $e^{\epsilon^2 p^2}$ is expanded in p^2 . We will be interested in the scattering length a and the effective range r , thus the expansion is terminated at $\mathcal{O}(p^4)$:

$$-\frac{1}{a} + \frac{1}{2} r p^2 + \mathcal{O}(p^4) = \left[-\frac{2\pi}{g^{(2)}} - \frac{1}{\pi} \frac{\sqrt{\pi}}{\epsilon} \left(1 - 2\epsilon p \left(\epsilon p - \frac{2}{3} \epsilon^3 p^3 \right) \right) \right] \left(1 + \epsilon^2 p^2 \right) + \mathcal{O}(p^4), \quad (\text{C14})$$

$$= -\left(\frac{2\pi}{g^{(2)}} + \frac{1}{\sqrt{\pi}\epsilon} \right) + \frac{1}{2} \left(\frac{2\epsilon}{\sqrt{\pi}} - \frac{4\pi\epsilon^2}{g^{(2)}} \right) p^2 + \mathcal{O}(p^4). \quad (\text{C15})$$

Note, that the momentum \vec{p} is the Jacobi momentum. The relation between the oscillator length for canonical relative coordinates and Jacobi coordinates is just a factor of $\sqrt{2}$ in the two-body sector and the oscillator lengths differ with the same factor. Therefore all lengths must be rescaled with $\sqrt{2}$ in order to get the canonical effective range expansion.

[1] E. Braaten, and H.-W. Hammer, Phys. Rept. **428**, 259 (2006) [arXiv:cond-mat/0410417].

- [2] V. Efimov, Phys. Lett. **33B**, 563 (1970).
- [3] P. F. Bedaque, H.-W. Hammer, and U. van Blocc, Phys. Rev. Lett. **82**, 463 (1999) [arXiv:nucl-th/9809025]; Nucl. Phys. A **646**, 444 (1999) [arXiv:nucl-th/9811046].
- [4] H.-W. Hammer, and L. Platter, Eur. Phys. J. A **32**, 113 (2007) [arXiv:nucl-th/0610105].
- [5] J. von Stecher, J. P. D’Incao, and C. H. Greene, Nature Physics **5**, 417 (2009) [arXiv:0810.3876].
- [6] G. J. Hanna, and D. Blume, Phys. Rev. A **74**, 063604 (2006).
- [7] J. von Stecher, Phys. Rev. Lett. **107**, 200402 (2011) [arXiv:1106.2319].
- [8] M. Gattobigio, A. Kievsky, and M. Viviani, Phys. Rev. A **84**, 052503 (2011) [arXiv:1106.3853].
- [9] A. N. Nicholson, Phys. Rev. Lett. **109** (2012) 073003 [arXiv:1202.4402].
- [10] F. Ferlaino, and R. Grimm, Physics **3**, 9 (2010).
- [11] C. Chin, R. Grimm, P. Julienne, and E. Tiesinga, Rev. Mod. Phys. **82**, 1225 (2010) [arXiv:0812.1496].
- [12] A. Zenesini et al., [arXiv:1205.1921].
- [13] D. Blume, Rep. Prog. Phys. **75**, 46401 (2012) [arXiv:1111.0941].
- [14] T. Busch, B.-G. Englert, K. Rzazewski, and M. Wilkens, Found. Phys. **28**, 549 (1998).
- [15] S. Jonsell, H. Heiselberg, and C. J. Pethick, Phys. Rev. Lett. **89**, 250401 (2002).
- [16] F. Werner, and Y. Castin, Phys. Rev. Lett. **97**, 150401 (2006).
- [17] P. Shea, B. P. van Zyl, and R. K. Bhaduri, Am. J. Phys. **77**, 511 (2009) [arXiv:0807.2979].
- [18] N. T. Zinner, J. Phys. A: Math. Theor. **45**, 205302 (2012) [arXiv:1111.1565].
- [19] X. Chen, L. M. Guan, and S. Chen, Eur. Phys. J. D **64**, 459 (2011) [arXiv:1101.5074].
- [20] Z. Idziaszek, and T. Calarco, Phys Rev A. **71**, 50701 (2005) [arXiv:quant-ph/0410163].
- [21] J.-J. Liang, and C. Zhang Phys. Scr. **77**, 025302 (2008) [arXiv:0803.1341].
- [22] A. Farrell, Z. MacDonald, and B. P. van Zyl, J. Phys. A: Math. Theor. **45**, 45303 (2012) [arXiv:1107.2334].
- [23] I. Stetcu, B. R. Barrett, and U. van Kolck, Phys. Lett. B **653**, 358 (2007) [arXiv:nucl-th/0609023].
- [24] I. Stetcu, J. Rotureau, B. R. Barrett, and U. van Kolck, J. Phys. G **37**, 064033 (2010) [arXiv:0912.3015].
- [25] J. Rotureau, I. Stetcu, B. R. Barrett, and U. van Kolck, Phys. Rev. C **85**, 034003 (2012) [arXiv:1112.0267].
- [26] S. Tölle, H.-W. Hammer, and B. Metsch, Comptes Rendus Physique **12**, 59 (2011) [arXiv:1008.0551].
- [27] L. Platter, H.-W. Hammer, and U.-G. Meissner, Phys. Rev. A **70**, 052101 (2004) [arXiv:cond-mat/0404313].
- [28] I. Stetcu, J. Rotureau, B. R. Barrett, and U. van Kolck, Ann. Phys. **325**, 1644 (2010) [arXiv:1001.5071].
- [29] J. Rotureau, I. Stetcu, B. R. Barrett, M. C. Birse, and U. van Kolck, Phys. Rev. A **82**, 032711 [arXiv:1006.3820].
- [30] I. Stetcu, B. R. Barrett, U. van Kolck, and J. P. Vary, Phys. Rev. A **76**, 063613 (2007) [arXiv:0705.4335].
- [31] E. D. Jurgenson, P. Navrátil, and R. J. Furnstahl, Phys. Rev. C **83**, 034301 (2011) [arXiv:1011.4085].
- [32] G. Hagen, T. Papenbrock, D. J. Dean, and M. Hjorth-Jensen, Phys. Rev. C **82**, 034330 (2010) [arXiv:1005.2627].
- [33] S. A. Coon, M. I. Avetian, M. K. G. Kruse, U. van Kolck, P. Maris, and J. P. Vary, [arxiv:1205.3230].

- [34] H.-W. Hammer, A. Nogga, and A. Schwenk, [arXiv:1210.4273].
- [35] G. P. Lepage, [arXiv:nucl-th/9706029].
- [36] R. J. Furnstahl, private communication.
- [37] I. M. Delves in *Advances in Nuclear Physics*, Vol. 5, M. Baranger and E. Vogt (eds.), Plenum Press, New York (1972).
- [38] T. R. Schneider, *Phys. Lett.* **40B**, 439 (1972).
- [39] R. J. Furnstahl, G. Hagen, and T. Papenbrock *Phys. Rev. C* **86**, 031301 (2012) [arXiv:1207.6100].
- [40] F. Serwane, G. Zürn, T. Lompe, T.B. Ottenstein, A.N. Wenz, and S. Jochim, *Science* **332**, 6027 (2011) [arXiv:1101.2124].
- [41] D. A. Varshalovich, and I. A. Stegun, *Quantum Theory of Angular Momentum*, 2nd Edition, World Scientific Publishing (1988).